

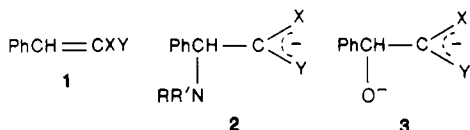
Kinetic Solvent Isotope Effect and Proton Inventory Study of the Carbon Protonation of Amine Adducts of Benzylidene Meldrum's Acid and Other Meldrum's Acid Derivatives. Evidence for Concerted Intramolecular Proton Transfer[†]

Claude F. Bernasconi,* Douglas E. Fairchild, and Christopher J. Murray

Contribution from the Thimann Laboratories of the University of California, Santa Cruz, California 95064. Received October 20, 1986

Abstract: Rate constants for carbon protonation of the glycinamide and morpholine adducts of benzylidene Meldrum's acid ($T_A^-(\text{gly})$ and $T_A^-(\text{mor})$) and of the anions of 5-benzyl and 5-(1-phenylethyl) Meldrum's acid (**13** and **14**) were determined in H_2O and D_2O . For protonation by L_3O^+ the kinetic solvent isotope effects for $T_A^-(\text{gly})$ and $T_A^-(\text{mor})$ are very low (0.82 and 0.72, respectively) and about threefold lower than those of **13** (2.48) and **14** (2.52); for protonation by $L_3^+NCH_2CONH_2$ the isotope effects are all normal, i.e., 6.01 for $T_A^-(\text{gly})$, 6.57 for **13**, and 7.68 for **14**. It is shown that the unusually low isotope effects for protonation of $T_A^-(\text{gly})$ and $T_A^-(\text{mor})$ by L_3O^+ are the result of a two-step mechanism which involves equilibrium protonation on the amine nitrogen, followed by rate limiting intramolecular proton switch from nitrogen to carbon. On the basis of this mechanism one may calculate a kinetic isotope effect for the intramolecular proton switch step of 3.66 ($T_A^-(\text{gly})$) and 3.29 ($T_A^-(\text{mor})$), respectively. Plausible alternative mechanisms such as carbon protonation by L_3O^+ with transition-state stabilization by hydrogen bonding between the amine nitrogen and L_3O^+ , or preequilibrium protonation on the amine nitrogen followed by rate-limiting carbon protonation by water, with transition-state stabilization by hydrogen bonding between the protonated amine nitrogen and the incipient hydroxide ion, are not consistent with the data. A proton inventory on the intramolecular proton switch step shows that the transition state includes a water molecule that acts as a bridge for the proton transfer. On the other hand, the proton inventory on the intermolecular protonation of $T_A^-(\text{gly})$ by $L_3^+NCH_2CONH_2$ indicates that the proton transfer is direct, in agreement with prevailing views.

The protonation of a carbon atom that is adjacent to a basic group such as an oxyanion or an amine poses an interesting mechanistic problem. We have encountered this problem on several occasions when dealing with Michael adducts between olefins of the type **1** and amines (**2**)¹⁻³ or hydroxide ion (**3**).^{4,5}



The mechanistic possibilities in aqueous solution are shown in Scheme I, where Z symbolizes the adjacent basic group. The charges shown correspond to the situation in **2**.

There are three major pathways for protonation at C^- (deprotonation at CH) for a given ionization state of Z. For the conversion of $Z-C^-$ into $Z-CH$, the three pathways are (1) direct carbon protonation of $Z-C^-$ ($k_1^{H_2O}$, k_1^H , k_1^{BH}), (2) rate-limiting protonation of the zwitterion HZ^+-C^- ($k_2^{H_2O}$, k_2^H , k_2^{BH}) with K_a^\pm acting as preequilibrium and K_a^+ as postequilibrium, and (3) rate-limiting intramolecular proton switch (k_i) with K_a^\pm acting as a preequilibrium. The mechanistic details of the intramolecular reaction will be discussed below.

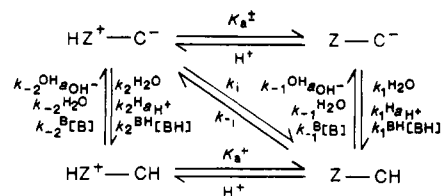
If all pathways contribute to the reaction, the pseudo-first-order rate constant is given by eq 1. Of the seven terms in eq 1 five

$$k_{\text{obsd}} = k_1^{H_2O} + k_1^H a_{H^+} + \frac{k_2^{H_2O}}{K_a^\pm} a_{H^+} + \frac{k_i}{K_a^\pm} a_{H^+} + \frac{k_2^H}{K_a^\pm} a_{H^+}^2 + k_1^{BH}[BH] + \frac{k_2^{BH}}{K_a^\pm} a_{H^+}[BH] \quad (1)$$

have a unique concentration dependence and can thus, at least in principle, easily be distinguished and evaluated experimentally. On the other hand, the second, third, and fourth terms all have the same dependence on a_{H^+} and hence cannot be distinguished on the basis of the rate law.

[†] This paper is dedicated to Professor Heinrich Zollinger on the occasion of his retirement from his chair at the Swiss Federal Institute of Technology (ETH).

Scheme I



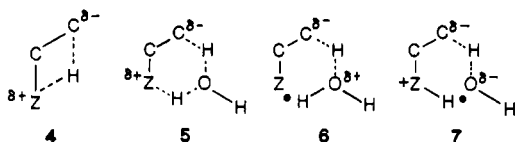
In order to facilitate the following discussion we shall define a phenomenological second-order rate constant for the sum of these three terms, k_H , as

$$k_H = k_1^H + \frac{k_2^{H_2O}}{K_a^\pm} + \frac{k_i}{K_a^\pm} \quad (2)$$

Evidence for the presence or absence of certain pathways contributing to k_H must be based on structure-reactivity relationships. For example, if the rate constants for the protonation of a comparable carbanion that lacks the Z group are known or can be estimated, this allows an estimate of k_1^H and $k_2^{H_2O}/K_a^\pm$ if K_a^\pm is also measurable. On this basis one can usually decide whether k_H may be entirely accounted for by k_1^H and/or $k_2^{H_2O}/K_a^\pm$, or whether there is a significant contribution by the k_i/K_a^\pm term. In other words, the presence of the intramolecular pathway (k_i) is inferred from a k_H value that is significantly higher than the expected value of $k_1^H + k_2^{H_2O}/K_a^\pm$.

The actual problem is more complex, though, because concerted intramolecular proton switch (k_i) is not the only mechanism involving the neighboring Z group that can lead to exalted k_H values. Structures 4-7 show four possible transition states which all could account for an exalted k_H value. **4** indicates direct intramolecular

- (1) Bernasconi, C. F.; Carré, D. *J. Am. Chem. Soc.* **1979**, *101*, 2698.
- (2) Bernasconi, C. F.; Fornarini, S. *J. Am. Chem. Soc.* **1980**, *102*, 5329.
- (3) (a) Bernasconi, C. F.; Murray, C. *J. Am. Chem. Soc.* **1984**, *106*, 3257. (b) Bernasconi, C. F.; Murray, C. *J. Am. Chem. Soc.* **1986**, *108*, 5257.
- (4) Bernasconi, C. F.; Leonarduzzi, G. *J. Am. Chem. Soc.* **1982**, *104*, 5143.
- (5) Bernasconi, C. F.; Fox, J. P.; Kanavarioti, A.; Panda, M. *J. Am. Chem. Soc.* **1986**, *108*, 2372.



proton transfer from ZH to C⁻ while **5** shows concerted intramolecular transfer involving a water bridge; either of these could be responsible for k_i although **5** seems more likely when Z and C⁻ are separated by only one or two carbon atoms (see Discussion).

6 represents carbon protonation by H₃O⁺ with transition-state stabilization through hydrogen bonding with Z; if Z is negatively charged there may also be additional stabilization by an electrostatic effect. The intramolecularly assisted pathway through **6** needs to be distinguished from simple, unassisted carbon protonation by H₃O⁺ (k_1^H in Scheme I) and hence the symbol k_{1i}^H will be used for its constant.

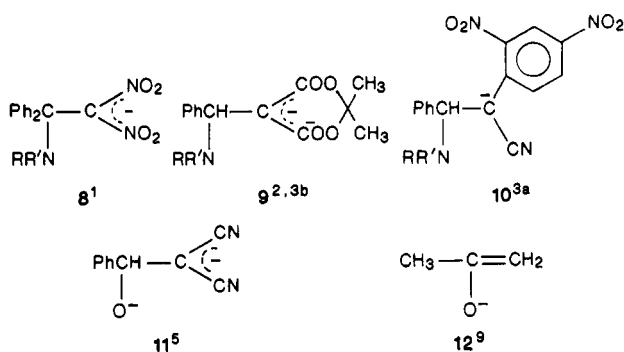
7 shows carbon protonation of HZ⁺-C⁻ by water, with transition-state stabilization through hydrogen bonding (and electrostatic attraction for positive ZH⁺) to the incipient hydroxide ion. Again, to distinguish this process from the unassisted $k_2^{H_2O}$ pathway we add the subscript *i* ($k_{2i}^{H_2O}$).

The above considerations show that k_H is really the sum of five rather than three terms (eq 3). The various pathways represented

$$k_H = k_1^H + k_{1i}^H + \frac{k_2^{H_2O}}{K_a^\pm} + \frac{k_{2i}^{H_2O}}{K_a^\pm} + \frac{k_i}{K_a^\pm} \quad (3)$$

by these terms are most easily visualized by means of the More O'Ferrall-Jencks⁶⁻⁸ diagram in Figure 1. The outer square in the figure refers to the unassisted pathways k_1^H (top horizontal axis) and $k_2^{H_2O}$ (bottom horizontal axis), the inner square shows the hydrogen bonding pathways, k_{1i}^H and $k_{2i}^{H_2O}$, while the concerted pathway (k_i) proceeds through the inside of the inner square.

A number of recently investigated systems in which C⁻ and Z are separated by only one carbon atom (**8-12**) have shown exalted k_H values, implying intramolecular assistance of one kind or another.



Jencks,^{9,10} who found an enhanced k_H value for the protonation of **12**, favors a transition state similar to that of **6** (intramolecular hydrogen bonding between O⁻ and H₃O⁺). In our studies of **8-11**, and most recently for **9**, we have advocated transition state **5**, based on the following reasoning. With primary aliphatic amine adducts of benzylidene Meldrum's acid (**9**) k_H increases with increasing basicity of the RR'N moiety. This increase can be described by a Brønsted β_N value of 0.29.^{3b} If **6** were the correct transition state, implying $k_H = k_{1i}^H$, the β_N value would be a measure of the hydrogen bonding interaction between the amine nitrogen and the hydronium ion which is in the process of delivering a proton to carbon. The value of 0.29 is, however, considerably higher than the expected $\beta_N \lesssim 0.16$ for such hydrogen bonding,^{3b} making **6** an unattractive proposal.

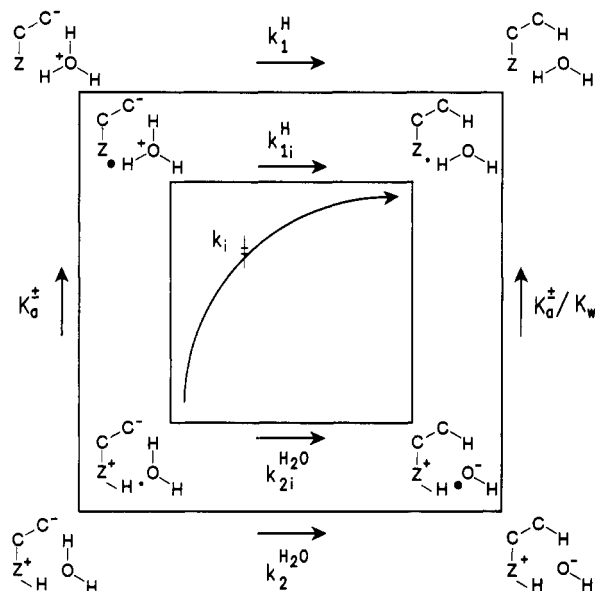
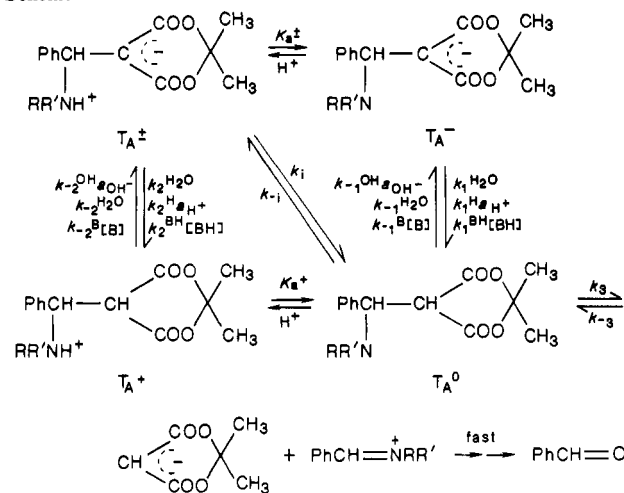


Figure 1. More O'Ferrall-Jencks diagram showing the different mechanistic possibilities for k_H (eq 3). The outer square refers to the unassisted pathways of Scheme I. The inner square shows the three possible mechanisms for intramolecular assistance. The reaction through the inside of the square is the concerted intramolecular proton transfer (k_i , **5**). The pathways along the edges of the inner square involve hydrogen bonding stabilization of the respective transition states (**6** for k_{1i}^H , **7** for $k_{2i}^{H_2O}$); the large dots indicate strong, the small dots weak, hydrogen bonding in the corner states of the inner square.

Scheme II



Alternatively, if **7** were the correct transition state, implying $k_H = k_{2i}^{H_2O}/K_a^\pm$, the β_N value of 0.29 would be equivalent to an $\alpha_N = 0.71$ for hydrogen bonding between the protonated amine nitrogen and the incipient hydroxide ion in **7**. Such a high α_N value is completely unrealistic¹¹ and firmly excludes **7**.

In the case of **11** studied in 50% and 70% aqueous Me₂SO the k_{1i}^H pathway was excluded because it requires k_{1i}^H values which are several orders of magnitude higher than the limit for a diffusion-controlled reaction, and the $k_{2i}^{H_2O}$ pathway was found unattractive because the magnitude of k_H requires an unreasonably strong hydrogen bond in the transition state (**7**).⁹

(11) Brønsted coefficients for transition-state stabilization by hydrogen bonding are usually in the range of 0.05 to 0.26, and mainly from 0.05 to 0.20.¹²⁻¹⁶

(12) Sayer, J. M.; Edman, C. *J. Am. Chem. Soc.* **1979**, *101*, 3010.

(13) Cox, M. M.; Jencks, W. P. *J. Am. Chem. Soc.* **1981**, *103*, 572.

(14) Kresge, A. J.; Tang, Y. C. *J. Chem. Soc., Chem. Commun.* **1980**, 309.

(15) Gilbert, H. F.; Jencks, W. P. *J. Am. Chem. Soc.* **1977**, *99*, 7931.

(16) Young, P. R.; Jencks, W. P. *J. Am. Chem. Soc.* **1977**, *99*, 1206.

(6) More O'Ferrall, R. A. *J. Chem. Soc. B* **1970**, 274.

(7) Jencks, W. P. *Chem. Rev.* **1972**, *72*, 705.

(8) Jencks, D. A.; Jencks, W. P. *J. Am. Chem. Soc.* **1977**, *99*, 7948.

(9) Tapuhi, E.; Jencks, W. P. *J. Am. Chem. Soc.* **1982**, *104*, 5758.

(10) Bednar, R. A.; Jencks, W. P. *J. Am. Chem. Soc.* **1985**, *107*, 7126.

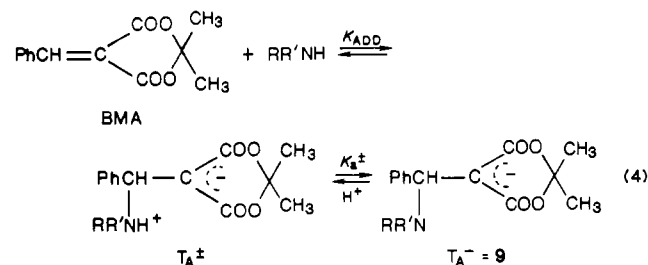
Table I. pK_a Values of Morpholine, Glycinamide, and the Morpholine and Glycinamide Adducts of Benzylidene Meldrum's Acid in H_2O and H_2O-D_2O Mixtures at $25^\circ C^a$

n^b	glycinamide	$T_A^\pm(\text{gly})$	morpholine	$T_A^\pm(\text{Mor})$
0	8.20 ± 0.01^c	8.00 ± 0.02^c	8.78 ± 0.01^c	8.80 ± 0.02^c
0.24	8.31 ± 0.01			
0.48	8.47 ± 0.01			
0.64	8.57 ± 0.01			
0.99	8.84 ± 0.01	8.65 ± 0.02	9.41 ± 0.01	9.46 ± 0.02

^a $\mu = 0.5$ M (KCl). ^bMole fraction D_2O . ^cReference 3a.

The present paper provides new and more conclusive evidence favoring transition state **5** in the protonation of the glycinamide and morpholine adducts of benzylidene Meldrum's acid (BMA). This evidence is based on kinetic solvent isotope effects and a proton inventory.

Amine adducts of BMA are among the most suitable for such studies because the equilibrium for amine addition, eq 4, strongly favors the adducts T_A^\pm and/or T_A^- over BMA even at relatively



low amine concentrations. Hence it is possible to directly measure rates of hydrolytic conversion of T_A^\pm or T_A^- to form benzaldehyde and Meldrum's acid (anion) as shown in Scheme II.

Since formation of T_A^0 is rate limiting,^{2,3b} k_{obsd} is given by eq 5, with k_H defined by eq 3.

$$k_{\text{obsd}} = k_1^{H_2O} + k_H a_{H^+} + \frac{k_2^H}{K_a^\pm} a_{H^+}^2 + k_1^{BH} [BH] + \frac{k_2^{BH}}{K_a^\pm} a_{H^+} [BH] \quad (5)$$

Results

pK_a Determinations. pK_a values of morpholine and glycinamide in D_2O and of glycinamide in various H_2O-D_2O mixtures were determined by potentiometric techniques as described in the Experimental Section. The pK_a values are summarized in Table I. pK_a^\pm values of the glycinamide and morpholine adducts of BMA (also in Table I) were measured spectrophotometrically as described previously.²

Kinetic Experiments. General Features. Rates of hydrolysis of T_A^\pm or T_A^- derived from BMA and glycinamide or morpholine were measured in H_2O , D_2O , and H_2O-D_2O mixtures (glycinamide adduct only). For purposes of comparison protonation rates in H_2O and D_2O of the Meldrum's acid derivatives **13** and **14** were also determined (see eq 8). All experiments were conducted in amine buffers or in HCl (DCI) solutions at $25^\circ C$. The ionic strength was kept constant at 0.5 M with KCl.

Hydrolysis of the Glycinamide and Morpholine Adducts of BMA in D_2O . The reactions were conducted in glycinamide and morpholine buffers, respectively. Rates were measured by monitoring the formation of benzaldehyde and the anion of Meldrum's acid at 255 nm. Pseudo-first-order rate constants were determined as a function of buffer concentration at different buffer ratios. The raw data are summarized in Tables S1 and S2¹⁷ (33 rate constants). They are consistent with eq 6^{3b} (with $L = D$ and k_L as in eq 3), i.e., under the reaction conditions the $k_2^{BL} a_{L^+} [BL^+] / K_a^\pm$ and $k_2^L a_{L^+}^2 / K_a^\pm$ terms (eq 5) are negligible.

$$k_{\text{obsd}} = \frac{K_a^\pm}{K_a^\pm + a_{L^+}} (k_1^{L_2O} + k_L a_{L^+} + k_1^{BL} [BL^+]) \quad (6)$$

(17) See paragraph concerning supplementary material at the end of this paper.

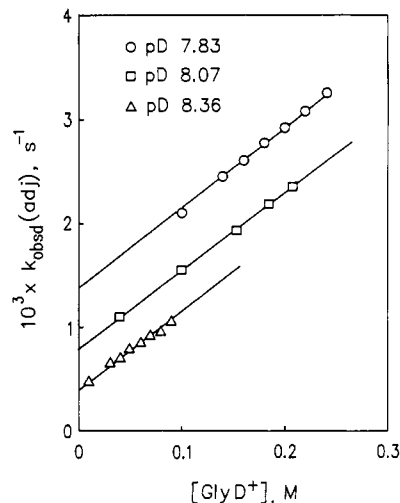


Figure 2. Reaction $T_A^-(\text{gly})$ in glycinamide buffers in D_2O . Plots according to eq 7 with $BL^+ = \text{glyD}^+$.

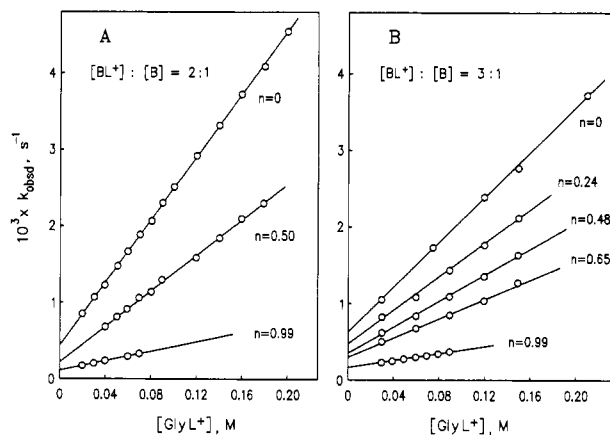


Figure 3. Reaction of $T_A^-(\text{gly})$ in glycinamide buffers at various mole fractions (n) of D_2O . Plots according to eq 6 with $[BL^+] = [\text{glyL}^+]$.

Table II. Rate Constants for the Lyonium Ion (k_L) and $RR'NL_2^+$ (k_1^{BL}) Catalyzed Conversion of T_A^- to T_A^0

	$T_A^-(\text{gly})$	$T_A^-(\text{mor})$
$k_H, M^{-1} s^{-1}$	$7.01 \pm 0.18 \times 10^4^a$	$5.58 \pm 0.15 \times 10^5^a$
$k_D, M^{-1} s^{-1}$	$8.56 \pm 0.35 \times 10^4$	$7.76 \pm 0.67 \times 10^5$
k_H/k_D	0.82 ± 0.06	0.72 ± 0.10
$k_1^{BH}, M^{-1} s^{-1}$	$4.54 \pm 0.20 \times 10^{-2}^{a,b}$	$6.83 \pm 0.75 \times 10^{-4}^{a,c}$
$k_1^{BD}, M^{-1} s^{-1}$	$7.65 \pm 0.15 \times 10^{-3}^b$	d
k_1^{BH}/k_1^{BD}	6.01 ± 0.38	d

^aReference 3b. ^bBH = glyH^+ , $BD^+ = \text{glyD}^+$. ^cBH = morH^+ , $BD = \text{morD}^+$. ^dToo small for accurate determination.

Figure 2 shows plots for the glycinamide adduct according to the rearranged eq 7. The intercepts are directly proportional to

$$k_{\text{obsd}}(\text{adj}) = k_{\text{obsd}} \frac{K_a^\pm + a_{L^+}}{K_a^\pm} = k_1^{L_2O} + k_L a_{L^+} + k_1^{BL} [BL^+] \quad (7)$$

a_{L^+} , indicating that $k_1^{L_2O}$ is negligible in the pL range investigated. k_L and k_1^{BL} in both H_2O and D_2O are summarized in Table II.

With the morpholine adduct the slopes of the buffer plots in D_2O (not shown) were very small and no meaningful k_1^{BL} value could be obtained. This reflects the previously noted^{3b} unusually large k_L for this adduct; because of the relatively larger isotope effect on k_1^{BL} than on k_L (see below) the k_1^{BL}/k_L ratio in D_2O becomes so small that buffer catalysis is too weak to measure.

Hydrolysis of the Glycinamide Adduct in H_2O-D_2O Mixtures (Proton Inventory). In a first series of experiments the hydrolysis was studied at 0, 0.50, and 0.99 mole fraction of D_2O . The same $[BL^+]:[B] = 2:1$ glycinamide buffer ratio was used in all solvent

Table III. Hydrolysis of Glycinamide Adduct in H₂O–D₂O Mixtures at 25 °C.^a Slopes and Intercepts of Plots of k_{obsd} vs. [BL⁺]

n^b	pL ^c	$10^4 \times$ intercept, ^d s ⁻¹	$10^4 \times$ slope, ^d M ⁻¹ s ⁻¹
[BL ⁺]:[B] = 2:1			
0	7.86	4.36 ± 0.11	205.1 ± 1.0
0.50	8.13	2.25 ± 0.16	115.4 ± 1.4
0.99	8.46	1.11 ± 0.01	31.13 ± 1.22
[BL ⁺]:[B] = 3:1			
0	7.72	6.01 ± 0.29	148 ± 2.5
0.24	7.83	4.46 ± 0.37	110 ± 4.1
0.48	7.99	3.36 ± 0.26	84.5 ± 3.0
0.64	8.09	2.98 ± 0.28	62.2 ± 2.8
0.99	8.36	1.47 ± 0.036	23.4 ± 0.6

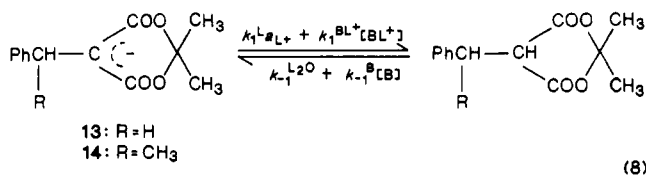
^a $\mu = 0.5$ M (KCl). ^bMole fraction of D₂O. ^cpL determined as described in the Experimental Section. ^dError limits are standard deviations.

mixtures. The results are summarized in Table S3¹⁷ (29 rate constants) while plots of k_{obsd} vs. [BL⁺] are shown in Figure 3A. The slopes and intercepts of these plots are summarized in Table III.

In a second series of experiments rates were determined at $n = 0, 0.24, 0.48, 0.64,$ and 0.99 and a [BL⁺]:[B] ratio of 3:1. The raw data are in Table S4¹⁷ (27 rate constants) while the slopes and intercepts of plots of k_{obsd} vs. [BL⁺] (Figure 3B) are included in Table III.

The data obtained in the first series were more reproducible and resulted in smaller standard deviations of slopes and intercepts. Hence more weight was given to the results of the first series (see Discussion).

Kinetics of Proton Transfer Involving 5-Benzyl and 5-(1-Phenylethyl) Meldrum's Acid in H₂O and D₂O. Proton transfer rates were measured in LCl and in glycinamide buffers. The reactions can be represented by eq 8.¹⁸



For the runs in LCl solutions the respective carbanion was first generated in 10⁻⁴ M KOL and then mixed with the acid solution in the stopped-flow apparatus. The data are summarized in Table S5¹⁷ (22 rate constants). Plots (not shown) of the observed pseudo-first-order rate constants vs. a_{L^+} gave excellent straight lines according to eq 9. The k_1^{L} and $k_{-1}^{\text{L}_2\text{O}}$ values are summarized

$$k_{\text{obsd}} = k_1^{\text{L}}a_{\text{L}^+} + k_{-1}^{\text{L}_2\text{O}} \quad (9)$$

in Table IV; since the intercepts ($k_{-1}^{\text{L}_2\text{O}}$) were quite small, more accurate values of $k_{-1}^{\text{L}_2\text{O}}$ were obtained by combining k_1^{L} with the photometrically determined $\text{p}K_{\text{a}}$ values. It is these $k_{-1}^{\text{L}_2\text{O}}$ values which are listed in Table IV.

The results for the runs in glycinamide buffers are summarized in Table S6¹⁷ (20 rate constants). In these experiments the equilibrium lies completely on the side of the carbanion and thus the slopes of plots of k_{obsd} vs. [B] are given by k_{-1}^{B} . The k_{-1}^{B} values and k_1^{BL} , calculated from k_{-1}^{B} and the $\text{p}K_{\text{a}}$ difference between the carbon acid and glycinamide, are included in Table IV.

Discussion

Kinetic Solvent Isotope Effects. Tables II and IV summarize rate and equilibrium constants for various proton transfers in H₂O and D₂O. Since the isotope effects are the main concern in the present context, the ones most relevant to our discussion have been collected in Table V for easy comparison.

(18) The $k_1^{\text{L}_2\text{O}}$ and $k_{-1}^{\text{OL}^-}a_{\text{OL}^-}$ terms are negligible under our experimental conditions.

Table IV. Rate Constants and $\text{p}K_{\text{a}}$ Values for Proton Transfers Involving 5-Benzyl Meldrum's Acid (13) and 5-(1-Phenylethyl) Meldrum's Acid (14) in H₂O and D₂O at 25 °C^a

constant	5-benzyl Meldrum's acid (13)	5-(1-phenylethyl) Meldrum's acid (14)
$k_1^{\text{H}}, \text{M}^{-1} \text{s}^{-1}$	$7.85 \pm 0.14 \times 10^4$	$3.73 \pm 0.07 \times 10^4$
$k_1^{\text{D}}, \text{M}^{-1} \text{s}^{-1}$	$3.16 \pm 0.05 \times 10^4$	$1.48 \pm 0.02 \times 10^4$
$k_1^{\text{H}}/k_1^{\text{D}}$	2.48 ± 0.09	2.52 ± 0.08
$k_{-1}^{\text{H}_2\text{O}}, \text{s}^{-1}$	35.0 ± 1.4	6.49 ± 0.16
$k_{-1}^{\text{D}_2\text{O}}, \text{s}^{-1}$	4.17 ± 0.12	0.776 ± 0.020
$k_{-1}^{\text{H}_2\text{O}}/k_{-1}^{\text{D}_2\text{O}}$	8.39 ± 0.58	8.36 ± 0.42
$k_1^{\text{BH}}, \text{M}^{-1} \text{s}^{-1}$	$8.05 \pm 0.53 \times 10^{-1}$	$4.36 \pm 0.20 \times 10^{-1}$
$k_1^{\text{BD}}, \text{M}^{-1} \text{s}^{-1}$	$1.23 \pm 0.01 \times 10^{-1}$	$0.568 \pm 0.027 \times 10^{-1}$
$k_1^{\text{BH}}/k_1^{\text{BD}}$	6.57 ± 0.45	7.68 ± 0.51
$k_{-1}^{\text{B}}(\text{H}_2\text{O}), \text{M}^{-1} \text{s}^{-1}$	$5.70 \pm 0.11 \times 10^4$	$1.20 \pm 0.05 \times 10^4$
$k_{-1}^{\text{B}}(\text{D}_2\text{O}), \text{M}^{-1} \text{s}^{-1}$	$1.12 \pm 0.01 \times 10^4$	$0.206 \pm 0.002 \times 10^4$
$k_{-1}^{\text{B}}(\text{H}_2\text{O})/k_{-1}^{\text{B}}(\text{D}_2\text{O})$	5.10 ± 0.12	5.82 ± 0.09
$\text{p}K_{\text{a}}(\text{H}_2\text{O})$	3.35 ± 0.01	3.76 ± 0.01
$\text{p}K_{\text{a}}(\text{D}_2\text{O})$	3.88 ± 0.01	4.28 ± 0.01
$\text{p}K_{\text{a}}(\text{D}_2\text{O}) - \text{p}K_{\text{a}}(\text{H}_2\text{O})$	0.53 ± 0.02	0.52 ± 0.02

^a $\mu = 0.5$ M (KCl). ^bFrom k_1^{L} and $\text{p}K_{\text{a}}$. ^cFrom k_{-1}^{B} and $\text{p}K_{\text{a}}$ values.

Table V. Kinetic Solvent Isotope Effects for Carbon Protonation of Various Meldrum's Acid Anions by L₃O⁺ and glyL⁺

acid	T _A ⁻ (gly)	T _A ⁻ (mor)	13	14
L ₃ O ⁺	0.82 ± 0.06^a	0.72 ± 0.10^a	2.48 ± 0.09^c	2.52 ± 0.08^c
glyL ⁺	6.01 ± 0.38^b		6.57 ± 0.45^d	7.68 ± 0.51^d

^a $k_{\text{H}}/k_{\text{D}}$, Table II. ^b $k_1^{\text{BH}}/k_1^{\text{BD}}$, Table II. ^c $k_1^{\text{H}}/k_1^{\text{D}}$, Table IV. ^d $k_1^{\text{BH}}/k_1^{\text{BD}}$, Table IV.

The most striking feature which emerges from Table V is the very low solvent isotope effects for the protonation of the BMA adducts by the lyonium ion ($k_{\text{H}}/k_{\text{D}} = 0.82$ and 0.72 for T_A⁻(gly) and T_A⁻(mor), respectively). These isotope effects are approximately threefold lower than those for the protonation of 13 and 14 by the lyonium ion. Since 13 and 14 are structurally very similar to T_A⁻ except that they lack the adjacent amine moiety, we conclude that the small isotope effects are the consequence of the mechanistic change induced by the amine moiety.

This conclusion is further supported by the fact that the isotope effect for the protonation of T_A⁻(gly) by the general acid glyL⁺ is normal (see below) and roughly the same as for the protonation of 13 and 14 by glyL⁺. This similarity in the isotope effects reflects the expectation that protonation by a buffer acid (k_1^{BL}) should not be significantly affected by the amine moiety in T_A⁻.

The question remains which mechanism for intramolecular assistance is most consistent with the low $k_{\text{H}}/k_{\text{D}}$ values. Our previous work^{3b} excluded the $k_{21}^{\text{H}_2\text{O}}/K_{\text{a}}^{\pm}$ pathway (transition state 7) altogether and rendered the k_{11}^{H} pathway (6) rather unattractive, without firmly excluding it, though. We show now that the low $k_{\text{H}}/k_{\text{D}}$ values are essentially inexplicable in terms of the k_{11}^{H} pathway.

A kinetic solvent isotope effect can be approximated as the product of a primary and a secondary isotope effect,¹⁹⁻²¹ eq 10. The secondary isotope effect may be expressed by eq 11 where

$$\left[\frac{k_{\text{H}_2\text{O}}}{k_{\text{D}_2\text{O}}} \right]_{\text{total}} = \left[\frac{k_{\text{H}_2\text{O}}}{k_{\text{D}_2\text{O}}} \right]_{\text{prim}} \left[\frac{k_{\text{H}_2\text{O}}}{k_{\text{D}_2\text{O}}} \right]_{\text{sec}} \quad (10)$$

ϕ_i^{R} and ϕ_j^{P} are the fractionation factors of those reactant and

$$\left[\frac{k_{\text{H}_2\text{O}}}{k_{\text{D}_2\text{O}}} \right]_{\text{sec}} = \left[\frac{\prod_i \phi_i^{\text{R}}}{\prod_j \phi_j^{\text{P}}} \right]^x \quad (11)$$

(19) Schowen, R. L. *Prog. Phys. Org. Chem.* **1972**, *9*, 275.

(20) (a) Kresge, A. J. *Pure Appl. Chem.* **1964**, *8*, 243. (b) Loughton, P. M.; Robertson, R. E. In *Solute-Solvent Interactions*; Coetzee, J. F., Ritchie, C. D., Eds.; Dekker: New York, 1969; p 400.

(21) (a) Schowen, K. B. J. In *Transition States of Biochemical Processes*; Gandour, R. D., Schowen, R. L., Eds.; Plenum Press: New York, 1978; p 225. (b) Schowen, R. L.; Schowen, K. B. J. *Methods Enzymol.* **1982**, *87*, 551.

product protons, respectively, which are not in flight, and χ is a progress variable of the reaction that is frequently equated with the Brønsted α or β value.^{19,21}

We first consider protonation by glyL^+ ($k_{\text{L}_2\text{O}} = k_1^{\text{BL}}$). With $\phi_{\text{N}^+\text{-L}}^{\text{R}} = 0.97^{19}$ and $\phi_{\text{N}^+\text{-L}}^{\text{P}} = 0.92^{19}$ eq 11 becomes

$$\left[\frac{k_{\text{H}_2\text{O}}}{k_{\text{D}_2\text{O}}} \right]_{\text{sec}} = \left[\frac{k_1^{\text{BH}}}{k_1^{\text{BD}}} \right]_{\text{sec}} = \left[\frac{0.97}{0.92} \right]^{\chi} \quad (12)$$

Using $\chi = \alpha = 0.55^{3b}$ affords $(k_1^{\text{BH}}/k_1^{\text{BD}})_{\text{sec}} = 1.03$. From this we estimate $(k_1^{\text{BH}}/k_1^{\text{BD}})_{\text{prim}} = (k_1^{\text{BH}}/k_1^{\text{BD}})_{\text{total}}/(k_1^{\text{BH}}/k_1^{\text{BL}})_{\text{sec}} \approx 6.01/1.03 = 5.83$ for $\text{T}_A^-(\text{gly})$, $\approx 6.57/1.03 = 6.38$ for **13**, and $\approx 7.68/1.03 = 7.46$ for **14**. These values fall within the normal range for primary kinetic isotope effect.²²

For protonation of **13** and **14** by L_3O^+ ($k_{\text{L}_2\text{O}} = k_1^{\text{L}}$) eq 11 becomes eq 13 with $\phi_{\text{O}^+\text{-L}}^{\text{R}} = 0.69^{19}$ and $\phi_{\text{O}^+\text{-L}}^{\text{P}} = 1.0^{19}$. If the

$$\left[\frac{k_{\text{H}_2\text{O}}}{k_{\text{D}_2\text{O}}} \right]_{\text{sec}} = \left[\frac{k_1^{\text{H}}}{k_1^{\text{D}}} \right]_{\text{sec}} = \left[\frac{0.69}{1} \right]^{2\chi} \quad (13)$$

same χ is chosen as for protonation by glyL^+ (0.55), this affords $(k_1^{\text{H}}/k_1^{\text{D}})_{\text{sec}} = 0.66$ and suggests $(k_1^{\text{H}}/k_1^{\text{D}})_{\text{prim}}$ values of 3.76 and 3.82, respectively. The reason why these primary effects are significantly lower than those for protonation by glyL^+ may be due to several factors. One is the relative weakness of the $\text{O}^+\text{-L}$ bond, as attested to by its low fractionation factor, $\phi_{\text{O}^+\text{-L}}^{\text{R}} = 0.69$.

Another is the larger $|\Delta pK|$ value in the L_3O^+ reactions ($|\Delta pK| = pK_a^{\text{CH}} - pK_a^{\text{H}_3\text{O}^+} = 5.10$ for **13**, 5.51 for **14**) compared to the $|\Delta pK|$ values in the glyL^+ -catalyzed reactions ($|\Delta pK| = pK_a^{\text{glyH}^+} - pK_a^{\text{CH}} = 4.85$ for **13**, 4.44 for **14**). It is well-known that primary kinetic isotope effects for proton transfers tend to reach a maximum around $|\Delta pK| = 0$ and to fall off for $|\Delta pK| > 0$.²²⁻²⁴ In this context one may understand the still lower $k_1^{\text{H}}/k_1^{\text{D}}$ ratios for 2,4-pentanedionate (1.4),²⁵ 3-methyl-2,4-pentanedionate (1.0),²⁶ and 2-acetylcyclohexanoate ion (1.7)²⁷ as being a consequence of still larger ΔpK values.

A third contributing factor to $(k_1^{\text{H}}/k_1^{\text{D}})_{\text{prim}}$ being lower than $(k_1^{\text{BH}}/k_1^{\text{BL}})_{\text{prim}}$ could be that $\chi = \alpha$ is too small for the hydronium ion catalyzed reaction. For example, if $\chi = 0.8$ instead of 0.55 we obtain $(k_1^{\text{H}}/k_1^{\text{D}})_{\text{sec}} = 0.55$ and hence $(k_1^{\text{H}}/k_1^{\text{D}})_{\text{prim}} \approx 4.51$ and 4.58, respectively.

Turning now to the protonation of T_A^- by L_3O^+ , we need to explain why the measured isotope effects, $k_{\text{H}}/k_{\text{D}}$, are so much lower (0.82 and 0.72, respectively) than those for the protonation of **13** and **14** by L_3O^+ (2.48 and 2.52, respectively). It is not obvious how hydrogen bonding with L_3O^+ in **6** could significantly lower the primary isotope effect. In fact it might be argued that inasmuch as hydrogen bonding probably increases the pK_a of L_3O^+ , this would reduce $\Delta pK = pK_a^{\text{CH}} - pK_a^{\text{L}_3\text{O}^+}$ and hence increase the primary isotope effect. We thus conclude that the low values of $k_{\text{H}}/k_{\text{D}}$ have to be a consequence of a very low secondary isotope effect in the order of 0.2. The secondary isotope effect (eq 11) for the reaction proceeding via **6** is given by eq 14,

$$\left[\frac{k_{\text{H}_2\text{O}}}{k_{\text{D}_2\text{O}}} \right]_{\text{sec}} = \left[\frac{k_{\text{H}}}{k_{\text{D}}} \right]_{\text{sec}} = \left[\frac{\phi_{\text{O}^+\text{-L}}^{\text{free}}}{1} \right]^{\chi} \left[\frac{\phi_{\text{O}^+\text{-L}}^{\text{Hb}}}{1} \right]^{\chi} \quad (14)$$

with $\phi_{\text{O}^+\text{-L}}^{\text{free}}$ referring to the non-hydrogen bonded hydron and $\phi_{\text{O}^+\text{-L}}^{\text{Hb}}$ to the hydrogen bonded (to Z) hydron in **6**. Using the usual value of 0.69¹⁹ for $\phi_{\text{O}^+\text{-L}}^{\text{free}}$ and assuming $\chi = 0.8$ would require a $\phi_{\text{O}^+\text{-L}}^{\text{Hb}} \approx 0.2$. This is a completely unrealistic value

in aqueous solution although fairly low (~ 0.3 to 0.4) fractionation factors are possible in non-aqueous solvents.²⁸ We therefore reject **6** as a viable transition state.

It should be noted that our findings and conclusion are very similar to the ones reached by Kresge²⁹ for the intramolecularly assisted hydrolysis of prostacyclin.

Having excluded **6** and **7**, the only remaining alternatives are **4** and **5**, i.e., $k_{\text{H}} = k_i/K_a^{\pm}$. From $k_{\text{H}}/k_{\text{D}}$ and $pK_a^{\pm}(\text{D}_2\text{O}) - pK_a^{\pm}(\text{H}_2\text{O})$ (Table I) one may calculate $k_i(\text{H}_2\text{O})/k_i(\text{D}_2\text{O})$ as

$$\frac{k_i(\text{H}_2\text{O})}{k_i(\text{D}_2\text{O})} = \frac{k_{\text{H}} K_a^{\pm}(\text{H}_2\text{O})}{k_{\text{D}} K_a^{\pm}(\text{D}_2\text{O})} \quad (15)$$

This affords $k_i(\text{H}_2\text{O})/k_i(\text{D}_2\text{O}) = 3.66 \pm 0.44$ for $\text{T}_A^-(\text{gly})$ and 3.29 ± 0.55 for $\text{T}_A^-(\text{mor})$.

Just as for protonation by glyL^+ , the secondary isotope effect on k_i should be very close to unity, regardless of whether the reaction proceeds through **4** or **5**. This implies that the above ratios essentially represent primary isotope effects. These isotope effects are about 40% smaller than those for protonation by glyL^+ . Likely reasons why these isotope effects are relatively small include the nonlinearity of the possible transition states^{22b,24,31} and a lack of transition-state symmetry^{24,30} which is implied by the Brønsted α_{N} value of 0.71^{3b} for k_i (which contrasts with $\alpha = 0.55$ for the intermolecular protonation by RNH_3^{+3b}).

Proton Inventory. The proton inventory study was carried out to determine whether or not the transition state of the k_i process includes a water molecule (**4** vs. **5**). **4** has actually not been seriously advocated because of the unfavorable geometry of the four-membered ring. In fact most transition states proposed for intramolecular proton transfers between two centers separated by very few atoms have included at least one or sometimes several water molecules.^{32,33} However, Menger³⁴ has recently questioned the common assumption of linearity in the transition state of proton transfers which implies that **4** may not be as unfavorable as commonly assumed.

Because the conclusions that can be drawn from proton inventories are very sensitive to experimental error,²¹ special precautions were taken to assure good reproducibility and internal consistency of our results. This is particularly important because the k_1 and k_1^{BL} values are not directly measurable but are obtained from intercepts and slopes, respectively, of plots of k_{obsd} vs. $[\text{BL}^+]$ (Figure 3). In particular, the experiments in pure water and pure D_2O were repeated in order to have strictly comparable conditions with the $\text{H}_2\text{O}-\text{D}_2\text{O}$ mixtures. The number of data points in any particular solvent was also generally higher than that for the simple isotope effect experiments, thus reducing the standard deviations in the intercept and slope values.

Because in any given series the buffer ratio $[\text{BL}^+]:[\text{B}]$ was kept constant in all solvents, the simple relationships of eq 16 and 17 (derived in the Appendix) hold if one assumes that $K_a^{\pm}/K_a^{\text{BL}}$ is independent of n . Since the latter assumption holds for $n = 0$

$$\frac{k_1^{\text{BL}}(n)}{k_1^{\text{BL}}(n=0)} = \frac{\text{slope}(n)}{\text{slope}(n=0)} \quad (16)$$

$$\frac{k_i(n)}{k_i(n=0)} = \frac{\text{intercept}(n)}{\text{intercept}(n=0)} \quad (17)$$

vs. $n = 0.99$ (Table I), it is reasonable to expect it to be valid at other n values as well.

Figure 4 shows the plots of $k_1^{\text{BL}}(n)/k_1^{\text{BL}}(n=0)$ vs. n for the two reaction series, and Figure 5 shows the plots of $k_i(n)/k_i(n=0)$

(22) Melander, L.; Saunders, W. H., Jr. *Reaction Rates of Isotopic Molecules*; Wiley-Interscience: New York, 1980; (a) p 133, (b) p 42.

(23) Bell, R. P. *The Proton in Chemistry*; Cornell University: Ithaca, NY, 1973; p 265.

(24) More O'Ferrall, R. A. In *Proton Transfer Reactions*; Caldin, E. F., Gold, V. Eds.; Wiley: New York, 1975; p 201.

(25) Long, F. A.; Watson, D. J. *Chem. Soc.* **1958**, 2019.

(26) Dahlberg, D. B.; Long, F. A. *J. Am. Chem. Soc.* **1973**, *95*, 3825.

(27) Riley, T.; Long, F. A. *J. Am. Chem. Soc.* **1962**, *84*, 522.

(28) Kreevoy, M. M.; Liang, T. M. *J. Am. Chem. Soc.* **1980**, *102*, 3315.

(29) Chiang, Y.; Cho, M. J.; Euser, B. A.; Kresge, A. J. *J. Am. Chem. Soc.* **1986**, *108*, 4192.

(30) Westheimer, F. H. *Chem. Rev.* **1961**, *61*, 265.

(31) Hawthorne, M. F.; Lewis, E. S. *J. Am. Chem. Soc.* **1958**, *80*, 4296.

(32) Gandour, R. D. *Tetrahedron Lett.* **1974**, 295.

(33) Kirby, A. L.; Lloyd, G. J. *J. Chem. Soc., Perkin Trans. 2* **1976**, 1762.

(34) (a) Menger, F. M.; Chow, J. F.; Kaiserman, H.; Vasquez, P. C. *J. Am. Chem. Soc.* **1983**, *105*, 4996. (b) Menger, F. M. *Tetrahedron* **1983**, *39*, 1013.

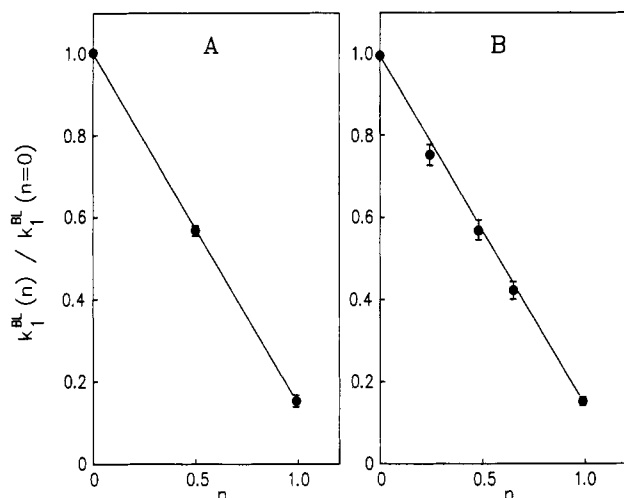


Figure 4. Proton inventories for k_1^{BL} at $[\text{BL}^+]:[\text{B}] = 2:1$ (A) and $[\text{BL}^+]:[\text{B}] = 3:1$ (B). Straight line plots indicate presence of a single active proton ($m = 1$) in the transition state.

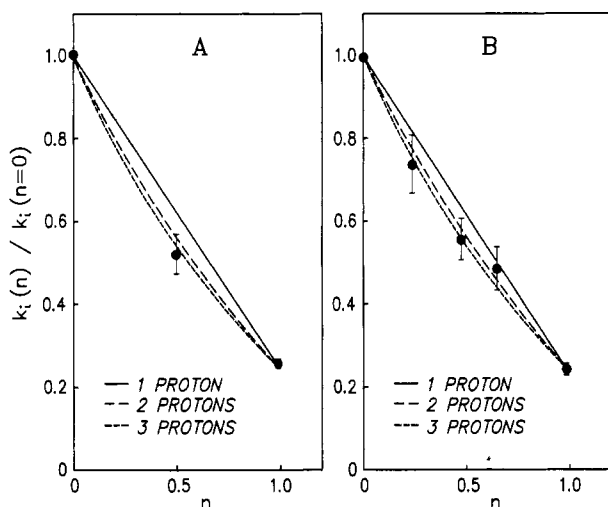


Figure 5. Proton inventory for k_i at $[\text{BL}^+]:[\text{B}] = 2:1$ (A) and $[\text{BL}^+]:[\text{B}] = 3:1$ (B). Curved lines are calculated for transition states with 2 and 3 active protons ($m = 2$ or 3), respectively.

0). It is apparent that for k_i the plots show a bowing down which is characteristic for transition states that contain more than one active proton,¹⁹⁻²¹ while for k_1^{BL} the plots are straight, indicating the presence of only one active proton.¹⁹⁻²¹ This latter finding is consistent with the general view that proton transfers from nitrogen or oxygen acids to carbon are direct and do not involve a solvent bridge.^{35,36}

For the k_i process an analysis in terms of the simplest form of the Gross-Butler equation,¹⁹⁻²¹ i.e., the one in which the transition state fractionation factors of the active protons (ϕ_T) are all assumed equal (eq 18), provides the results summarized in Table VI. Because the series conducted at a buffer ratio $[\text{BL}^+]:[\text{B}]$

$$\frac{k_i(n)}{k_i(n=0)} = (1 - n + n\phi_T)^m \quad (18)$$

= 2:1 resulted in better reproducibility and smaller standard deviations than the one at a 3:1 ratio, we shall rely more heavily on the former.³⁹ Entry 1 in the table refers to the experimental

Table VI. Proton Inventory of k_i -Step. Analysis by the Gross-Butler Equation

entry	parameter	$[\text{BL}^+]:[\text{B}] = 2:1$	$[\text{BL}^+]:[\text{B}] = 3:1$
1	$k_i(n = 0.99)/k_i(n = 0)$	0.255 ± 0.008	0.245 ± 0.017
2	ϕ_T for $m = 1$	0.247 ± 0.009	0.237 ± 0.017
3	ϕ_T for $m = 2$	0.500 ± 0.010	0.490 ± 0.018
4	ϕ_T for $m = 3$	0.630 ± 0.007	0.622 ± 0.014
	$k_i(n = 0.50)^a/k_i(n = 0)$		
5	calcd for $m = 1$	0.624 ± 0.004	0.634 ± 0.008
6	calcd for $m = 2$	0.563 ± 0.007	0.570 ± 0.014
7	calcd for $m = 3$	0.541 ± 0.007	0.549 ± 0.013
8	obsd value	0.516 ± 0.049	0.559 ± 0.067

^aIn the $[\text{BL}^+]:[\text{B}] = 3:1$ buffer $k_i(n = 0.48)/k_i(n = 0)$.

$k_i(n = 0.99)/k_i(n = 0)$ ratios. Entries 2-4 are the ϕ_T values calculated from the experimental $k_i(n = 0.99)/k_i(n = 0)$ ratios by applying eq 18. Entries 5-7 represent the predicted $k_i(0.50)/k_i(n = 0)$ ratios for various m values while entry 8 gives the observed $k_i(n = 0.50)/k_i(n = 0)$ ratios. Our analysis indicates that the observed $k_i(n = 0.50)/k_i(n = 0)$ ratios are consistent with either $m = 2$ or 3, i.e., either one or two water molecules in the transition state (dashed lines in Figure 5), but inconsistent with $m = 1$ (solid line in Figure 5).

Conclusions. Exalted rates for carbon protonation of amine adducts of BMA by H_3O^+ found in earlier work^{2,3b} indicate intramolecular assistance by the amine nitrogen. Four possible transition states which could account for this assistance are shown in 4-7, with the corresponding pathways shown in Figure 1. On the basis of Brønsted β_N values 7 was excluded previously.^{3b} In the present paper we were able to exclude 6 on the basis of the kinetic solvent isotope effect and 4 on the basis of a proton inventory study. Hence we conclude that the reaction proceeds through 5.

Protonation of 8, 10, 11, and similar compounds probably occurs via analogous transition states, but it is not clear whether our conclusions apply to the acetone enolate ion (12) as well. Since here the protonation site and the adjacent oxyanion are part of the same resonance system it is conceivable that a different mechanism (6?) may prevail.

One important difference between proton transfers involving a carbon acid or a carbanion and proton transfers from a normal acid to a normal base in aqueous solution is that the former occur directly^{35,36} and the latter via a water bridge.^{37,38} As recently shown by Jencks,³⁶ this strong preference for direct transfer when a carbon site is involved prevails even with cyanide ion which otherwise behaves almost like a normal base. The geometric disadvantage of 4 must therefore be quite severe to make proton transfer via a water bridge (5) the preferred pathway in our system. It would be interesting to see how large a ring size for the transition state is needed to restore the natural tendency of proton transfer at carbon to occur directly.

Experimental Section

Materials. Benzylidene Meldrum's acid was available from a previous study.² 5-Benzyl Meldrum's acid was prepared from Meldrum's acid⁴⁰ by the method of Hrubowchak and Smith,⁴¹ mp 80-80.5 °C (lit.⁴¹ mp 80-81 °C). 5-(1-Phenylethyl) Meldrum's acid was synthesized from benzylidene Meldrum's acid by the procedure of Haslego and Smith,⁴² mp 100-101 °C (lit.⁴² mp 104-105 °C). Morpholine, methoxyacetic acid (used as buffer for pK_a determinations), and glycine hydrochloride were purified as described before.⁴³ Other buffer materials were analytical grade commercial products. D_2O (Norell Inc.) was 99.9% pure

(35) (a) Hibbert, F. *Compr. Chem. Kinet.* **1977**, *8*, 97. (b) Albery, W. J. In *Proton Transfer Reactions*; Caldin, E. F., Gold, V., Eds.; Wiley: New York, 1975; p 285.

(36) Bednar, R. A.; Jencks, W. P. *J. Am. Chem. Soc.* **1985**, *107*, 7126 and references cited therein.

(37) Eigen, M. *Angew. Chem., Int. Ed. Engl.* **1964**, *1*, 3.

(38) Grunwald, E.; Eustace, D. In *Proton Transfer Reactions*; Caldin, E., Gold, V., Eds.; Chapman and Hall: London, 1975; pp 103-120.

(39) The uncertainties estimated for the various entries in Table VI actually slightly overestimate the actual errors because they are interdependent. In other words, the high limit for the calculated as well as the observed $k_i(n = 0.50)/k_i(n = 0)$ or $k_i(n = 0.48)/k_i(n = 0)$ values is based on the high limit of $k_i(n = 0.99)/k_i(n = 0)$ and the same is true for the respective low limits. This means, for example, that the high limit of $k_i(n = 0.50)/k_i(n = 0) = 0.565$ needs to be compared with the high limits of the calculated $k_i(n = 0.50)/k_i(n = 0)$ ratios (0.628 for $m = 1$; 0.570 for $m = 2$; 0.548 for $m = 3$).

(40) Davidson, D.; Bernhard, S. A. *J. Am. Chem. Soc.* **1948**, *70*, 3426.

(41) Hrubowchak, D. M.; Smith, F. X. *Tetrahedron Lett.* **1983**, *24*, 4951.

(42) Haslego, M. L.; Smith, F. X. *Synth. Commun.* **1980**, *10*, 421.

(43) Bernasconi, C. F.; Bunnell, R. D. *Isr. J. Chem.* **1985**, *26*, 420.

and DCl (Aldrich) 99% pure. KOD solutions were prepared by dissolving KOH in D₂O. Mixed isotopic waters were prepared gravimetrically, and the mole fraction of deuterium was checked by NMR with the method of Schowen.^{21b} Isotopic dilution from buffers was taken into account when preparing reaction solutions; it always amounted to less than 1%.

pH and pK_a Measurements. An Orion 611 digital pH meter with a Corning glass electrode (No. 476022) and a Beckman reference electrode (No. 39402) was used, with the solutions being thermostated at 25 °C. For the stopped-flow runs the pH was measured in mock-mixing experiments. In D₂O pD was obtained as pD = pH_{obsd} + 0.40⁴⁴ with pH_{obsd} being the value read from the pH meter. Calibration curves of pL - pH_{obsd} vs. mole fraction of D₂O (*n*) in H₂O/D₂O mixtures were obtained by measuring pH_{obsd} of 0.002 M LCl solutions. Our calibration curve was in excellent agreement with that of Glasoe and Long.⁴⁴

pK_a values for 5-benzyl and 5-(1-phenylethyl) Meldrum's acid in H₂O and D₂O were measured by classical spectrophotometric procedures at 272 or 273 nm, while the pK_a values of morpholine and glycineamide in D₂O were determined potentiometrically.

Kinetic Measurements. The rates of the reactions of 5-benzyl and 5-(1-phenylethyl) Meldrum's acid were measured in a Durrum stopped-flow apparatus with computerized data analysis while all other kinetic measurements were carried out with a Perkin Elmer 559A double beam spectrophotometer. The *k*_{obsd} values reported in Tables S1-S6¹⁷ are in most cases the average of several runs.

Appendix

Derivation of Equations 16 and 17. According to eq 6 *k*₁^{BL}(*n*) can be expressed by eq 19 and *k*_L(*n*) by eq 20. Since the buffer ratio, *R* = [B]/[BL⁺], is kept constant in all H₂O/D₂O mixtures,

$$k_1^{BL}(n) = \left[1 + \frac{a_{L^+}}{K_a^\pm} \right]_n \text{slope}(n) \quad (19)$$

$$k_L(n) = \left[1 + \frac{a_{L^+}}{K_a^\pm} \right]_n \frac{\text{intercept}(n)}{a_{L^+}} \quad (20)$$

(44) Glasoe, P. K.; Long, F. A. *J. Phys. Chem.* 1960, 64, 188.

we can express *a*_{L⁺} as *K*_a^{BL}/*R* with *K*_a^{BL} being the acid dissociation constant of BL⁺. Equations 19 and 20 thus become

$$k_1^{BL}(n) = \left[1 + \frac{K_a^{BL}}{K_a^\pm} R \right]_n \text{slope}(n) \quad (21)$$

$$k_L(n) = \left[1 + \frac{K_a^{BL}}{K_a^\pm} R \right]_n \frac{\text{intercept}(n)}{K_a^{BL}(n)} R \quad (22)$$

If we now assume that *K*_a^{BL}/*K*_a[±] is independent of *n*, eq 23 and 24 follow from eq 21 and 22, respectively.

$$\frac{k_1^{BL}(n)}{k_1^{BL}(n=0)} = \frac{\text{slope}(n)}{\text{slope}(n=0)} \quad (23) = (16)$$

$$\frac{k_L(n)}{k_L(n=0)} = \frac{\text{intercept}(n)}{\text{intercept}(n=0)} \frac{K_a^{BL}(n=0)}{K_a^{BL}(n)} \quad (24)$$

By combining eq 15 and eq 24 we deduce eq 25, and assuming that *k*_L = *k*_i/*K*_a⁺

$$\frac{k_i(n)}{k_i(n=0)} = \frac{k_L(n)}{k_L(n=0)} \frac{K_a^\pm(n)}{K_a^\pm(n=0)} = \frac{\text{intercept}(n)}{\text{intercept}(n=0)} \frac{K_a^{BL}(n=0)}{K_a^{BL}(n)} \frac{K_a^\pm(n)}{K_a^\pm(n=0)} \quad (25)$$

Using again the assumption that *K*_a^{BL}/*K*_a[±] is independent of *n* simplifies eq 25 to eq 17.

Acknowledgment. This research was supported by Grant CHE-8315374 from the National Science Foundation.

Supplementary Material Available: All observed pseudo-first-order rate constants, Tables S1-S6 (6 pages). Ordering information is given on any current masthead page.

Timing of the Radical Recombination Step in Cytochrome P-450 Catalysis with Ring-Strained Probes

Paul R. Ortiz de Montellano* and Ralph A. Stearns

Contribution from the Department of Pharmaceutical Chemistry, School of Pharmacy, University of California, San Francisco, California 94143. Received October 29, 1986

Abstract: Nortricyclane, methylcyclopropane, and bicyclo[2.1.0]pentane have been used to probe the catalytic mechanism of microsomal cytochrome P-450. Nortricyclane is oxidized by rat liver microsomes to nortricyclanol without the detectable formation of norborn-5-en-2-ol. Methylcyclopropane is similarly oxidized to cyclopropylmethanol without the detectable formation of 3-buten-1-ol or cyclobutanol. The radical pair in the hydroxylation reaction therefore collapses faster than the cyclopropylmethyl radical rearranges (1 × 10⁸ s⁻¹). In contrast, microsomal oxidation of bicyclo[2.1.0]pentane yields approximately a 7:1 mixture of *endo*-2-hydroxybicyclo[2.1.0]pentane and 3-cyclopenten-1-ol. Deuterium labeling studies indicate the *endo* hydrogen is predominantly or exclusively removed from, and the hydroxyl group is delivered to, the *endo* face in both the rearranged and unrearranged products. The results indicate that a radical pair is formed in P-450-catalyzed hydroxylations that collapses with stereochemical specificity at a rate in excess of 1 × 10⁹ s⁻¹.

Cytochrome P-450 enzymes reductively activate molecular oxygen to a ferryl-bound species that inserts into unactivated carbon-hydrogen bonds.¹ The product of the reaction with a hydrocarbon is usually the corresponding alcohol. These reactions were first thought to occur by a concerted mechanism, but recent

evidence favors a nonconcerted mechanism in which hydrogen abstraction by the activated oxygen is followed by rapid collapse of the resulting radical or ion pair to give the hydroxylated product. Three lines of experimental evidence argue for a nonconcerted

* Address correspondence to Paul R. Ortiz de Montellano, School of Pharmacy, University of California, San Francisco, CA 94143

(1) Ortiz de Montellano, P. R. In *Cytochrome P-450: Structure, Mechanism, and Biochemistry*; Ortiz de Montellano, P. R., Ed.; Plenum: New York, 1986; pp 217-271.